J|A|C|S
ARTICLES

Toward π-Conjugated Molecule Bundles: Synthesis of a Series of *B,B′,B″*-Trianthryl-*N,N′,N″*-triarylborazines and the Bundle Effects on Their Properties

Atsushi Wakamiya, Toshihisa Ide, and Shigehiro Yamaguchi*

Contribution from the Department of Chemistry, Graduate School of Science,
Nagoya University, Chikusa, Nagoya 464-8602, Japan

Received June 7, 2005; E-mail: yamaguchi@chem.nagoya-u.ac.jp

Abstract: As a prototype of a π-conjugated molecule bundled system, a series of *B*,*B′*,*B″*-trianthryl- *N*,*N′*,*N″*-triarylborazine derivatives bearing various *p*-substituted phenyl groups (p-R$-$C$_6$H$_4$: R = hexyl (**1**), *i*-Pr (**2**), CF$_3$ (**3**), Br (**5**)) as aryl groups was designed and synthesized. The crystal structure analysis of these derivatives confirmed that the three anthryl and three phenyl groups are bundled up alternately in a C_3 symmetrical gear-shaped fashion. On the basis of this structure, the trianthrylborazine derivatives form a unique honeycomblike packing structure consisting of intermolecular π-stacking of the anthryl moieties. Significant bundle effects were observed in the photophysical and electrochemical properties of these compounds. In their fluorescence spectra, the trianthrylborazine derivatives (**1**−**3**) show intense emissions around 390 nm, whose quantum yields (**1**, $\Phi_F = 0.62$; **2**, $\Phi_F = 0.59$; **3**, $\Phi_F = 0.63$) are about twice high as that of anthracene ($\Phi_F = 0.27$). The cyclic voltammetry measurements show that the oxidation peak potential can be tuned by varying the substituents on the phenyl moieties. Theoretical calculations (B3LYP/ 6-31G-(d)) suggested that secondary through-bond/through-space interactions in the bundled structure play an important role in the tuning of these properties. Facile structural derivatization at the 10-position of the anthryl moieties of trianthrylborazine was conducted to demonstrate the utility of the borazine skeleton as a core framework for new organic electronic materials.

Introduction

Progress in organic electronics and optoelectronics highly relies on the creation of excellent new π-electron materials. One possible direction in molecular designs is the construction of cumulated π-conjugated systems in which multiple π-conjugated frameworks are assembled three-dimensionally through covalent bonding in a specific fashion. These systems are divided into several types such as (a) spiro-type, (b) propeller-type, and (c) double-decker-type (Figure 1), exemplified by spirofluorenes[1−3] and spirobiphenalenes,[4] metal-quinolinato complex such as Alq$_3$,[5] and paracyclophane-based materials,[6−9] respectively. In these π-electron systems, spatial proximity or topology among the π-conjugated moieties causes unique orbital interactions, which make it possible to tune the electronic structures (types (a)[1−4] and (c)[6−9]). In addition, the rigid three-dimensional skeletons favor the formation of well-oriented crystalline (type (a)[4]) or stable amorphous (types (a)[1−3] and (b)[5]) solid-state structures.

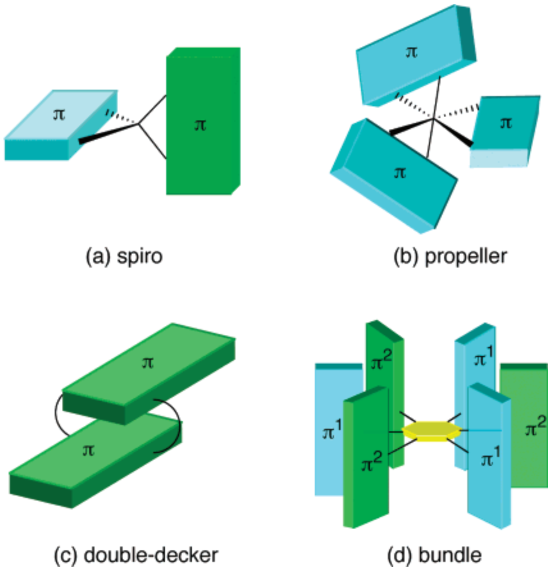

(a) spiro (b) propeller

(c) double-decker (d) bundle

Figure 1. Various types of cumulated π-conjugated systems.

We now focus our attention on another type of cumulated system, that is, π-conjugated molecule bundles with a hexagonal core, as shown in Figure 1d. In this system, six π-conjugated

---

(1) (a) Salbeck, J.; Yu, N.; Bauer, J.; Weissörtel, F.; Bestgen, H. *Synth. Met.* **1997**, *91*, 209. (b) Salbeck, J.; Weissörtel, F.; Bauer, J. *Macromol. Symp.* **1997**, *125*, 121. (c) Johansson, N.; Salbeck, J.; Bauer, J.; Weissörtel, F.; Bröms, P.; Andersson, A.; Salaneck, W. R. *Adv. Mater.* **1998**, *10*, 1136. (d) Steuber, F.; Staudigel, J.; Stössel, M.; Simmerer, J.; Winnacker, A.; Spreitzer, H.; Weissörtel, F.; Salbeck, J. *Adv. Mater.* **2000**, *12*, 130.

(2) (a) Wong, K.-T.; Chien, Y.-Y.; Chen, R.-T.; Wang, C.-F.; Lin, Y.-T.; Chiang, H.-H.; Hsieh, P.-Y.; Wu, C.-C.; Chou, C. H.; Su, Y. O.; Lee, G.-H.; Peng, S.-M. *J. Am. Chem. Soc.* **2002**, *124*, 11576. (b) Chien, Y.-Y.; Wong, K.-T.; Chou, P.-T.; Cheng, Y.-M. *Chem. Commun.* **2002**, 2874. (c) Wu, C.-C.; Liu, T.-L.; Hung, W.-L.; Hung, W.-Y.; Lin, Y.-T.; Wong, K.-T.; Chen, R.-T.; Chen, Y.-M.; Chien, Y.-Y. *J. Am. Chem. Soc.* **2003**, *125*, 3710. (d) Wu, C.-C.; Liu, T.-L.; Lin, Y.-T.; Hung, W.-Y.; Ke, T.-H.; Wong, K.-T.; Chao, T.-C. *Appl. Phys. Lett.* **2004**, *85*, 1172. (e) Fungo, F.; Wong, K.-T.; Ku, S.-Y.; Hung, Y.-Y.; Bard, A. J. *J. Phys. Chem. B* **2005**, *109*, 3984.

10.1021/ja0537171 CCC: $30.25 © 2005 American Chemical Society

frameworks are bundled up in parallel fashion. We envisioned that the construction of this bundled structure would cause certain through-bond and/or through-space interaction among the π-conjugated frameworks, resulting in the appearance of novel photophysical and electronic properties different from the original properties of each π-conjugated framework. Here, we employ borazine (B_3N_3) as the core skeleton. The use of borazine allows us not only to achieve efficient synthesis, but also to incorporate two kinds of π-conjugated frameworks, π^1 and π^2, alternately on the boron and nitrogen atoms, respectively, as shown in Figure 1. Although benzene might be the primarily conceivable candidate for the core skeleton,[10] difficulty is often encountered in the synthesis of such sterically congested trigonally symmetric benzenes in terms of efficiency and regioselectivity.[10e] The borazine skeleton has a definite advantage over the benzene skeleton in this point. As a prototype of the borazine-based bundle, we here report the synthesis and properties of a series of *B,B′,B″*-trianthryl-*N,N′N″*-triarylborazines. Our interests in this paper are the elucidation of bundle effects on the properties of these compounds as well as the investigation of their potential utility as a key framework for the creation of new organic electronic materials.

Scheme 1

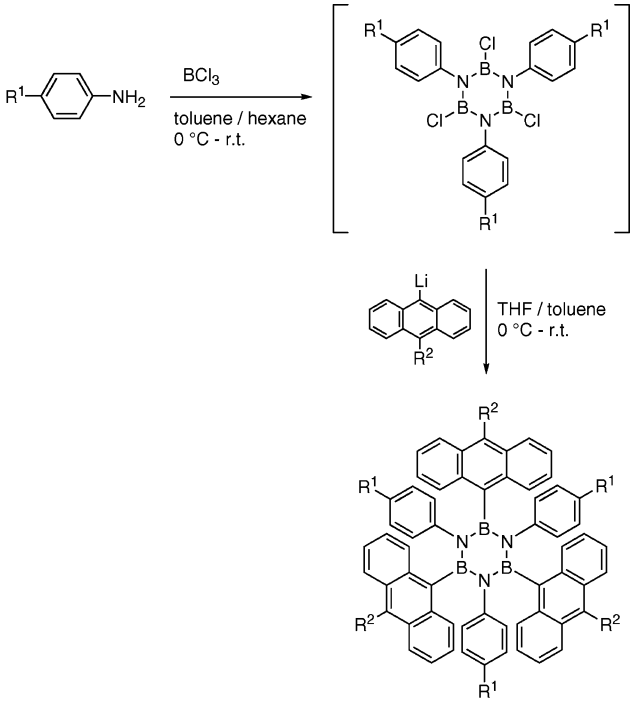

1: R^1 = hexyl, R^2 = H, 70%
2: R^1 = *i*-Pr, R^2 = H, 66%
3: R^1 = CF_3, R^2 = H, 33%
5: R^1 = hexyl, R^2 = Br, 70%

Results and Discussion

Synthesis of Trianthrylborazines. The trianthrylborazines were synthesized using a one-pot procedure, as shown in Scheme 1.[11] The reaction of BCl_3 with aniline derivatives produced the corresponding *B,B′,B″*-trichloro-*N,N′,N″*-triarylborazines, which were subsequently treated with 9-anthryllithium to afford a series of trianthrylborazines bearing various *p*-substituted phenyl groups ($p\text{-R}-\text{C}_6\text{H}_4$: R = hexyl (**1**), *i*-Pr (**2**), CF_3 (**3**)) as the aryl groups on the nitrogen atoms. Although the overall yield using this procedure was only moderate to good, the procedure is essentially facile and allows us to synthesize the bundled systems on a gram scale.

X-ray Crystal Structure Analysis. The crystal structures of the series of trianthrylborazines were determined by X-ray crystallography. As an example, the structure of the CF_3-substituted derivative **3** is shown in Figure 2. The crystal lattice of **3** belongs to the trigonal *R*-3 space group, and this compound has a 3-fold symmetry axis. The anthryl and phenyl groups are arranged nearly orthogonally to the borazine plane, but the dihedral angles between these planes and the borazine plane deviate slightly from 90°, at 75.6° and 72.4°, respectively. As a consequence, the six π-frameworks are arranged in propeller-like fashion.

There are two notable features. (1) The nonbonded distances between the ipso positions of the anthryl and phenyl groups

---

(3) (a) Yu, W.-L.; Pei, J.; Huang, W.; Heeger, A. J. *Adv. Mater.* **2000**, *12*, 828. (b) Bach, U.; Cloedt, K. D.; Spreitzer, H.; Gätzel, M. *Adv. Mater.* **2000**, *12*, 1060. (c) Marsitzky, D.; Murray, J.; Scott, J. C.; Carter, K. R. *Chem. Mater.* **2001**, *13*, 4285. (d) Chiang, C.-L.; Shu, C.-F. *Chem. Mater.* **2002**, *14*, 682. (e) Wu, F.-I.; Dodda, R.; Reddy, D. S.; Shu, C.-F. *J. Mater. Chem.* **2002**, *12*, 2893. (f) Katsis, D.; Geng, Y. H.; Ou, J. J.; Culligan, S. W.; Trajkovska, A.; Chen, S. H.; Rothberg, L. J. *Chem. Mater.* **2002**, *14*, 1332. (g) Kadashchuk, A.; Valhnin, A.; Skryshevski, Y.; Arkhipov, V. I.; Emelianova, E. V.; Bässler, H. *Chem. Phys.* **2003**, *191*, 243. (h) Schneider, D.; Rabe, T.; Riedl. T.; Dobbertin, T.; Kröger, M.; Becker, E.; Johannes, H.-H.; Kowalsy, W.; Weimann, T.; Wang, J.; Hinze, P. *Appl. Phys. Lett.* **2004**, *85*, 1659. (i) Chiang, C.-L.; Wu, M.-F.; Dai, D.-C.; Wen, Y.-S.; Wang, J.-K.; Chen, C.-T. *Adv. Funct. Mater.* **2005**, *15*, 231.

(4) (a) Chi, X.; Itkis, M. E.; Patrick, B. O.; Barclay, T. M.; Reed, R. W.; Oakley, R. T.; Cordes, A. W.; Haddon, R. C. *J. Am Chem. Soc.* **1999**, *121*, 10395. (b) Koutentis, P. A.; Chen, Y.; Cao, Y.; Best, T. P.; Itkis, M. E.; Beer, L.; Oakley, R. T.; Cordes, A. W.; Brock, C. P.; Haddon, R. C. *J. Am. Chem. Soc.* **2001**, *123*, 3864. (c) Chi, X.; Itkis, M. E.; Kirschbaum, K.; Pinkerton, A. A.; Oakley, R. T.; Cordes, A. W.; Haddon, R. C. *J. Am. Chem. Soc.* **2001**, *123*, 4041. (d) Itkis, M. E.; Chi, X.; Cordes, A. W.; Haddon, R. C. *Science* **2002**, *296*, 1443. (e) Chi, X.; Itkis, M. E.; Reed, R. W.; Oakley, R. T.; Cordes, A. W.; Haddon, R. C. *J. Phys. Chem. B* **2002**, *106*, 8278. (f) Huang, J.; Kertesz, M. *J. Am. Chem. Soc.* **2003**, *125*, 13334. (g) Pal, S. K.; Itkis, M. E.; Reed, R. W.; Oakley, R. T.; Cordes, A. W.; Tham, F. S.; Siegrist, T.; Haddon, R. C. *J. Am. Chem. Soc.* **2004**, *126*, 1478.

(5) (a) Tang, C. W.; VanSlyke, S. A. *Appl. Phys. Lett.* **1987**, *51*, 913. (b) Chen, C. H.; Shi, J. *Coord. Chem. Rev.* **1998**, *171*, 161. (c) Jeong, Y. S.; Troadec, D.; Moliton, A.; Ratier, B.; Antony, R.; Veriot, G. *Synth. Met.* **2002**, *127*, 195. (d) Cölle, M.; Gmeiner, J.; Milius, W.; Hillebrecht, H.; Brütting, W. *Adv. Funct. Mater.* **2004**, *13*, 108. (e) Braun, M.; Gmeiner, J.; Milius, W.; Hillebrecht, H.; Wendland, O.; Schütz, J. U.; Brütting, W. *J. Chem. Phys.* **2001**, *114*, 9625. (f) Brinkmann, M.; Gadret, G.; Muccini, M.; Taliani, C.; Masciocchi, N.; Sironi, A. *J. Am. Chem. Soc.* **2000**, *122*, 5147. (g) Lin, B. C.; Cheng, C. P.; You, Z.-Q.; Hsu, C.-P. *J. Am. Chem. Soc.* **2005**, *127*, 66.

(6) (a) Bartholomew, G. P.; Bazan, G. C. *Acc. Chem. Res.* **2001**, *34*, 30. (b) Oldham, W. J.; Miyao, Y.-J.; Lachicotte, R. J.; Bazan, G. C. *J. Am. Chem. Soc.* **1998**, *120*, 419. (c) Bazan, G. C.; Oldham, W. J.; Lachicotte, R. J.; Tretiak, S.; Chernyak, V.; Mukamel, S. *J. Am. Chem. Soc.* **1998**, *120*, 9188. (d) Wang, S.; Bazan, G. C.; Tretiak, S.; Mukamel, S. *J. Am. Chem. Soc.* **2000**, *122*, 1289. (e) Zyss, J.; Ledoux, I.; Volkov, S.; Chernyak, V.; Mukamel, S.; Bartholomew, G. P.; Bazan, G. C. *J. Am. Chem. Soc.* **2000**, *122*, 11956. (f) Bartholomew, G. P.; Ledoux, I.; Mukamel, S.; Bazan, G. C.; Zyss, J. *J. Am. Chem. Soc.* **2002**, *124*, 13480. (g) Bartholomew, G. P.; Rumi, M.; Pond, S. J. K.; Perry, J. W.; Tretiak, S.; Bazan, G. C. *J. Am. Chem. Soc.* **2004**, *126*, 11529.

(7) (a) Morisaki, Y.; Chujyo, Y. *Macromolecules* **2002**, *35*, 587. (b) Morisaki, Y.; Chujyo, Y. *Chem. Lett.* **2002**, 194. (c) Morisaki, Y.; Ishida, T.; Chujyo, Y. *Macromolecules* **2002**, *35*, 7872. (d) Morisaki, Y.; Chujyo, Y. *Macromolecules* **2003**, *36*, 9319. (e) Morisaki, Y.; Chujyo, Y. *Macromolecules* **2004**, *37*, 4099. (f) Morisaki, Y.; Chujyo, Y. *Bull. Chem. Soc. Jpn.* **2005**, *78*, 288.

(8) (a) Salhi, F.; Lee, B.; Metz, C.; Bottomley, L. A.; Collard, D. M. *Org. Lett.* **2002**, *4*, 3195. (b) Salhi, F.; Collard, D. M. *Adv. Mater.* **2003**, *15*, 81.

(9) (a) Guyard, L.; Nguyen Dinh An, M.; Audebert, P. *Adv. Mater.* **2001**, *13*, 133. (b) Guyard, L.; Audebert, P. *Electrochem. Commun.* **2001**, *3*, 164.

(10) (a) Kobayashi, K.; Shirasaka, T.; Sato, A.; Horn, E.; Furukawa, N. *Angew. Chem., Int. Ed.* **1999**, *38*, 3438. (b) Kobayashi, K.; Shirasaka, T.; Horn, E.; Furukawa, N. *Tetrahedron Lett.* **2000**, *41*, 89. (c) Kobayashi, K.; Sato, A.; Sakamoto, S.; Yamaguchi, K. *J. Am. Chem. Soc.* **2003**, *125*, 3035. (d) Kobayashi, K.; Kobayashi, N. *J. Org. Chem.* **2004**, *69*, 2487. (e) Traber, B.; Wolff, J. J.; Rominger, F.; Oeser, T.; Gleiter, R.; Goebel, M.; Wortmann, R. *Chem. Eur. J.* **2004**, *10*, 1227. (f) Rathore, R.; Burns, C. L.; Abdelwahed, S. A. *Org. Lett.* **2004**, *6*, 1689. (g) Jia, W.-L.; Wang, R.-Y.; Song, D.; Ball, S. J.; McLearn, A. B.; Wang, S. *Chem. Eur. J.* **2005**, *11*, 832.

(11) For the synthesis of hexaphenylborazine: Groszos, S. J.; Stafiej, S. F. *J. Am. Chem. Soc.* **1958**, *80*, 1357.

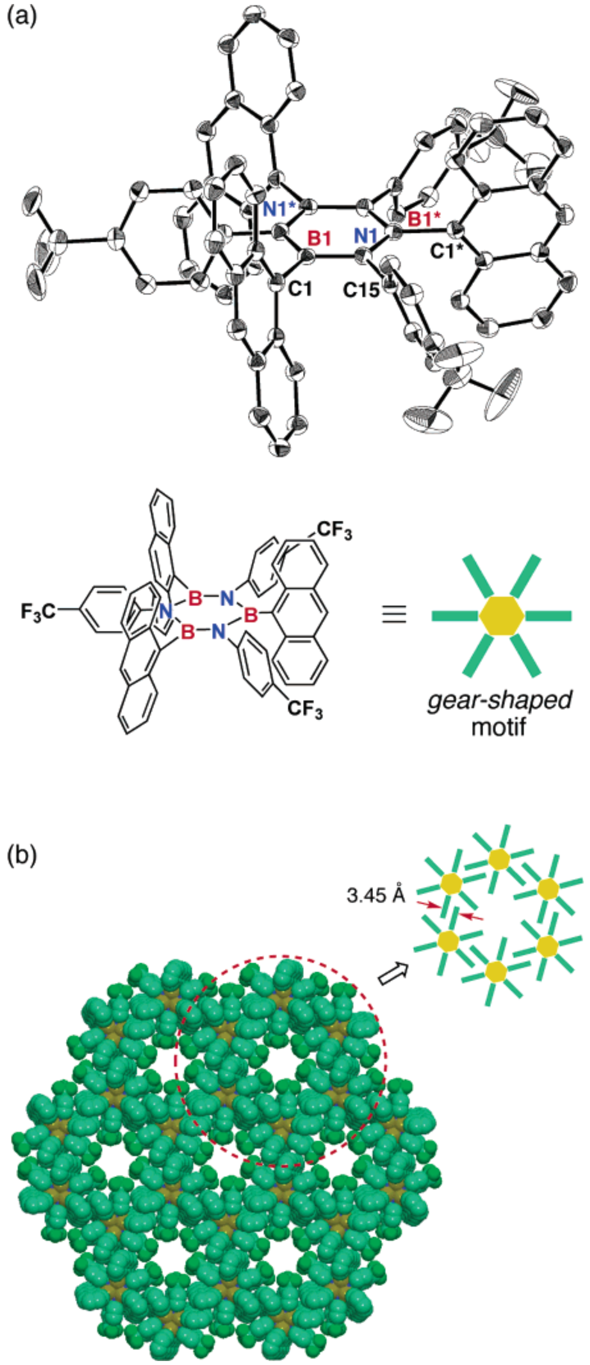

Figure 2. (a) ORTEP drawing of **3** (R = CF$_3$). Thermal ellipsoids are drawn at the 50% probability level. Hydrogen atoms and solvent molecules are omitted for clarity. Selected bond lengths (Å) and angles (deg) are as follows: N1−B1, 1.437(2); N1−B1*, 1.447(2); B1−C1, 1.581(3); N1−C15, 1.447(2); B1−N1−B1*, 122.86(16); B1−N1−C15, 119.40(14); B1*−N1−C15, 117.62(14); N1−B1−N1*, 117.14(14); N1−B1−C1, 123.39(15); N1*−B1−C1, 119.45(15). (b) Packing structure of **3** (R = CF$_3$). In the crystal structure of **3**, solvent molecules of hexane and toluene were included between the π-stacking network sheets. The inner space of each hexagonal assembly is occupied by a disordered hexane molecule. Solvent molecules and hydrogen atoms are omitted for clarity.

Table 1. Photophysical Data for a Series of *B*,*B*′,*B*″-Trianthrylborazine Derivatives

	absorption[a]	fluorescence[a]
compd.	λ_{max}/nm (log ε)	λ_{max}/nm (Φ_F)[b]
1	390 (4.41)	397 (0.62)
2	390 (4.43)	397 (0.59)
3	390 (4.45)	397 (0.63)
4	387 (4.49)	390 (0.38)
6	402 (4.58)	411 (0.80)[c]
7	437 (4.60)	466 (0.73)[d]
8	401 (4.66)	459 (0.36)[c]
anthracene	377 (3.77)	380 (0.27)

[a] In THF. [b] Determined with anthracene as a standard, unless otherwise stated. [c] Determined with 9,10-diphenylanthracene as a standard. [d] Determined with perylene as a standard.

Chart 1. Structure of *B*,*B*′,*B*″-Trianthryl-*N*,*N*′,*N*″-tributylborazine **4**

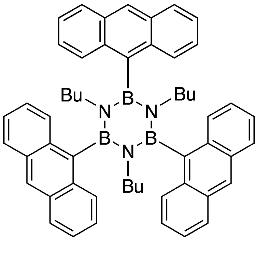

4

(C1−C15, C1*−C15) are rather shorter (3.00 and 2.90 Å) than the sum of the van der Waals radii of two C sp^2 atoms (3.45 Å), suggesting a possible through-space interaction between them. (2) The structure of **3** serves as a hexagonal gear-shaped motif, and in the crystal it forms a unique honeycomblike packing structure, as shown in Figure 2b. It is noteworthy that this two-dimensional network consists of offset face-to-face intermolecular π-stacking between the anthryl moieties with a cofacial π−π distance of about 3.45 Å. A similar packing structure is also observed for **2**, which indicates the generality of this packing structure for these C_3 symmetrical borazine derivatives. However the honeycomb network of **2** is rather loose compared to that of **3**, due to the bulkier isopropyl groups on the benzene rings (see Supporting Information).

Photophysical Properties. To investigate the effects of the bundled structure on the compounds' photophysical properties, we obtained UV−vis absorption and fluorescence spectra for compounds **1**−**3**. The data are collected in Table 1 together with the data for a parent anthracene and an *N*,*N*′,*N*″-trialkyl derivative **4** (Chart 1) for comparison.

In the UV−vis absorption spectra, all the trianthrylborazine derivatives **1**−**4** have absorption maxima around 387−390 nm, which are bathochromically shifted by about 10 nm from that of anthracene (377 nm), mainly due to the inductive electronic effect of the borazine moiety.

More significant differences were observed by comparing the fluorescence spectra of anthracene, *N*,*N*′,*N*″-trialkyl derivative **4**, and *N*,*N*′,*N*″-triaryl derivative **1**. The emission maximum shifts to longer wavelengths, in the order anthracene < **4** < **1**, by about 10−17 nm. Moreover, the fluorescence intensity significantly increases in the same order, as shown in Figure 3. In terms of the fluorescence quantum yield, more than a 2-fold increment was observed between the parent anthracene (Φ_F = 0.27) and the bundled molecule **1** (Φ_F = 0.62). This bundle effect can be rationalized by considering that the sterically congested bundled structure prevents conformational disorder leading to nonradiative decay from the excited state.

Cyclic Voltammetry Measurement. We also evaluated the electrochemical properties of the synthesized compounds by means of cyclic voltammetry. Their cyclic voltammograms are shown in Figure 4, and the data are summarized in Table 2.

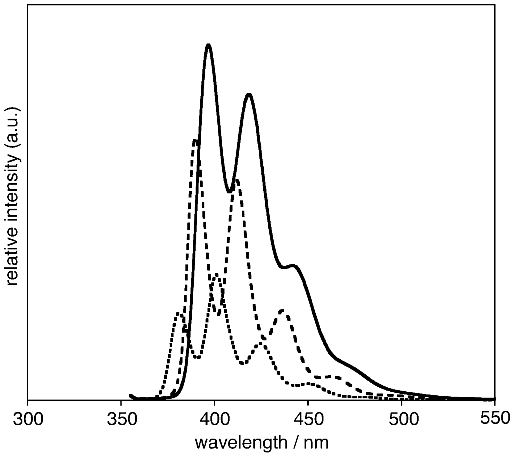

Figure 3. Fluorescence spectra of **1**, **4**, and anthracene in THF: solid line, **1**; dashed line, **4**; dotted line, anthracene.

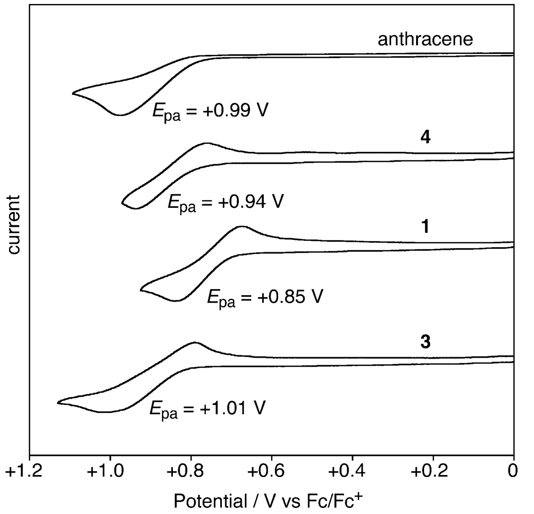

Figure 4. Cyclic voltammograms of anthracene, **4**, **1**, and **3** in CH_2Cl_2, measured with $Bu_4N^+ClO_4^-$ (0.1 M) as a supporting electrode at a scan rate of 100 mV s^{-1}.

Table 2. Oxidation Potentials[a] and KS HOMO Levels[b]

compd.	E_{pa}[c] (V)	KS HOMO (eV)
anthracene	+0.99	−5.23
4	+0.94	−5.09[d]
1	+0.85	−4.98[e]
3	+1.01	−5.31

[a] In CH_2Cl_2 containing $Bu_4N^+ClO_4^-$ (0.1 M) with a scan rate of 100 mV s^{-1}. [b] Calculated at the B3LYP/6-31G(d) level of theory. [c] V vs Fc/Fc$^+$. [d] Calculated for the model compound **4′**. [e] Calculated for the model compound **1′** (R = Me).

Again, bundle effects are noticeable in the comparison between anthracene, *N*,*N′*,*N″*-trialkyl derivative **4**, hexyl-substituted **1**, and CF_3-substituted **3** with respect to the reversibility of the redox process as well as oxidation potential. Thus, while the parent anthracene only showed an irreversible one-electron oxidation wave, all trianthrylborazines, **1**, **3**, and **4**, exhibited quasi-reversible one-electron oxidation waves, suggesting that the radical cations produced thereby can be stabilized in the trianthrylborazine structures. The oxidation peak potential (E_{pa}) gradually shifts to less positive potential in the order anthracene (+0.99 V vs Fc/ Fc$^+$) > **4** (+0.94 V) > **1** (+0.85 V). These results demonstrate that there is an interaction between the alternately bundled phenyl and anthryl moieties, resulting in the decrease in E_{pa} from anthracene to **1**. However, the CF_3-derivative **3** (+1.01 V) has a higher oxidation peak potential than **1**, indicating that the electronic structures can be tuned by varying the *p*-substituents of the phenyl moieties on the nitrogen atoms. This secondary perturbation may be beneficial to the material designs, since the electronic fine-tuning of the material is a key issue to fabricate high-performance multilayered electronic devices, such as organic light-emitting diodes.

Theoretical Calculations. To obtain a deeper insight into the bundle effects on the electronic structures, we conducted DFT calculations at the B3LYP/6-31G(d) level of theory. The calculated Kohn−Sham (KS) HOMO level of **1′** (R = Me, a model compound for **1**: −4.98 eV) is slightly higher than those of *B*,*B′*,*B″*-trianthryl-*N*,*N′*,*N″*-trimethylborazine **4′** (a model compound for **4**: −5.09 eV) and anthracene (−5.23 eV). In addition, a comparison between **1′** and **3** (R = CF_3, −5.31 eV) shows that the introduction of the electron-withdrawing CF_3 group decreases the HOMO level by 0.33 eV compared to that of **1′** (−4.98 eV). All these results are qualitatively in good agreement with the aforementioned cyclic voltammetry results. It is noteworthy that, while the HOMO of the trianthrylborazine is mainly localized on the three anthracene moieties, it also contains slight contributions from the B−N−B through-bond interaction as well as the through-space interaction between adjacent anthryl and phenyl moieties, as shown in Figure 5. These secondary through-bond/through-space interactions play an important role in the tuning of the electronic structures. In fact, as shown by comparison of the HOMOs of **1′** and **3**, the extent of the contribution of the benzene moieties is significantly decreased by the incorporation of the electron-withdrawing CF_3 group.

Structural Modification. One synthetic advantage of the present trianthrylborazine systems is their facile structural derivatization. In the one-pot synthesis of the trianthrylborazine framework, the use of 10-bromo-9-anthryllithium, instead of 9-anthryllithium, gave tris(10-bromoanthryl)borazine **5**, as shown in Scheme 1. This compound can be used as a key precursor for a variety of 10-substituted anthryl derivatives. For example, as shown in Scheme 2, the trilithiation of **5** using *t*-BuLi followed by treatment with electrophiles such as diisopropylsilyl chloride or dimesitylfluoroborane gave tris(diisopropylsilyl) derivative **6** and tris(dimesitylboryl) derivative **7**, respectively. In addition, after the transformation from **5** to the corresponding trizinc species, the Negishi coupling reaction with *p*-bromo(diphenylamino)benzene gave the triphenylamine-bound derivative **8**.

These extended bundle systems show some intriguing properties. The tris(diisopropylsilyl) derivative **6** shows a very intense fluorescence maximum at 411 nm with a fluorescent quantum yield of 0.80 (Figure 6). The higher quantum yield of **6** compared to that of **1** (Φ_F = 0.62) can be ascribed to the silyl effect on the fluorescence of anthracene.[12] The tris(dimesitylboryl)-substituted derivative **7** shows substantially red-shifted absorption and fluorescence maxima at 438 and 466 nm, respectively, due to the contribution of the vacant p-orbital of the boryl groups.[13b] These values are slightly longer, even in comparison with those of dimesityl(9-anthryl)borane[13] (absorp-

---

(12) Kyushin, S.; Ikarugi, M.; Goto, M.; Hiratsuka, H.; Matsumoto, H. *Organometallics* **1996**, *15,* 1067.

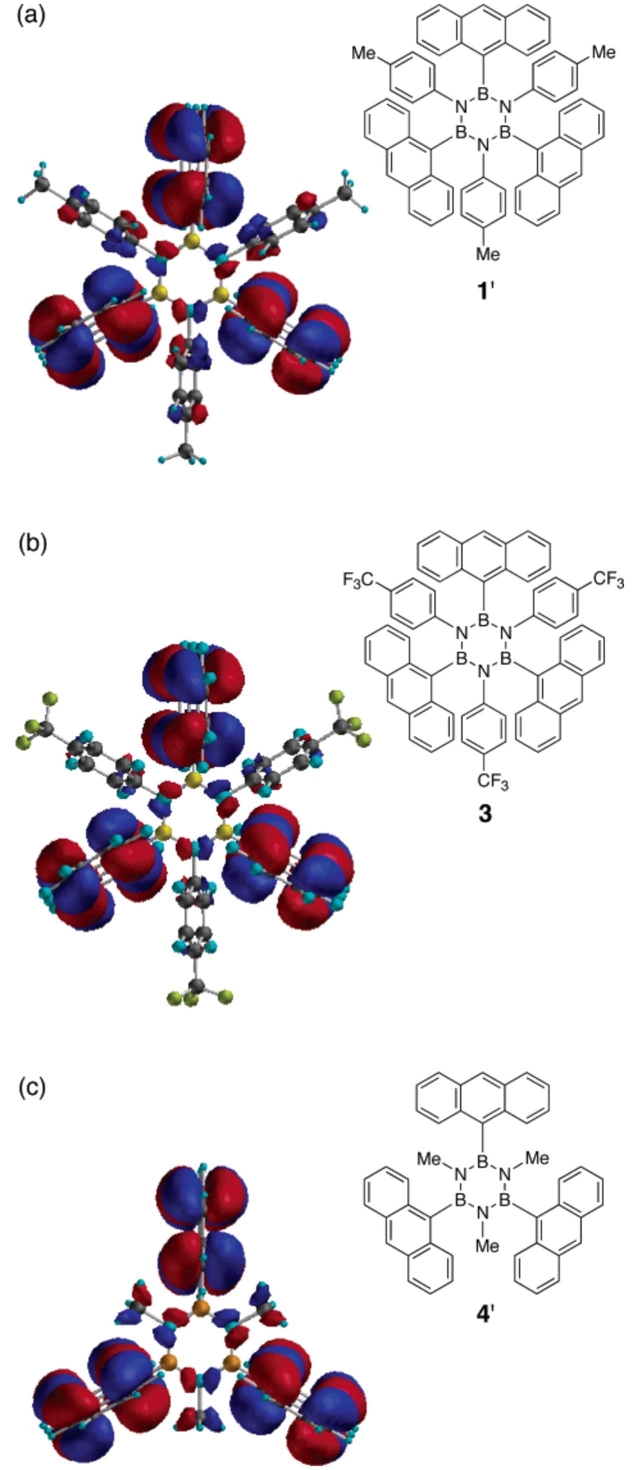

Figure 5. Pictorial presentation of KS HOMO of (a) **1′**, (b) **3**, and (c) **4′**.

Scheme 2[a]

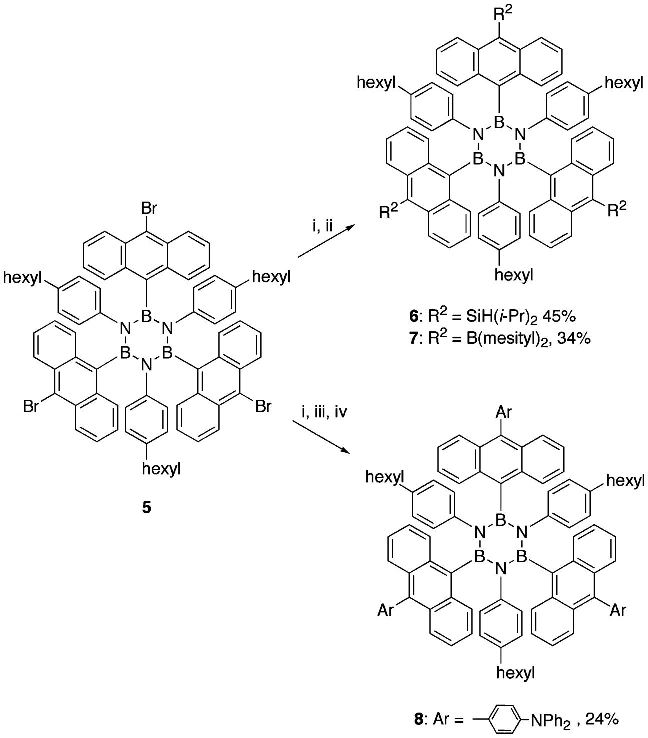

[a] Reagents and conditions: i, *t*-BuLi, THF; ii, H*i*-Pr$_2$SiCl or Mes$_2$BF; iii, ZnCl$_2$(tmen); iv, ArBr, Pd(PPh$_3$)$_4$, THF.

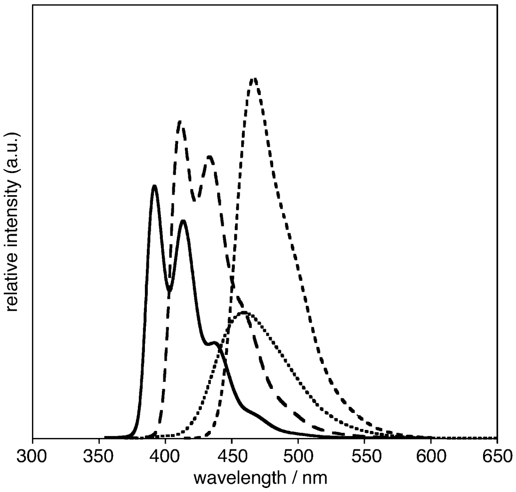

Figure 6. Fluorescence spectra of **1** and **6**−**8** in THF: solid line, **1**; long dashed line, **6**; short dashed line, **7**; dotted line, **8**.

tion, λ_{max} 420 nm; fluorescence λ_{max} 455 nm). In addition, the aminophenyl derivative **8** shows rather red-shifted emission at 459 nm, in comparison with that of the unsubstituted derivate **1**, while its absorption maximum is only slightly longer than that of **1**. These results suggest a substantial contribution of the aminophenyl group to the excited state.

Notably, in cyclic voltammetry, the boryl-substituted derivative **7** shows three reversible reduction waves with peak potential $E_{pc} = -2.29$, -2.41, and -2.52 V (vs Fc/Fc$^+$) in THF, as well as a reversible oxidation wave with potential $E_{pa} = +0.72$ V in CH$_2$Cl$_2$, as shown in Figure 7. The first reduction peak potential ($E_{pc}{}^1$; -2.29 V) of **7** is comparable to that of Alq$_3$ (-2.36 V),[14,15] which indicates its potential as an electron-transporting material for organic electroluminescence devices. In contrast, the aminophenyl derivative **8** shows three oxidation waves with peak potential $E_{pa} = +0.60$, $+0.80$, and $+1.03$ V (vs Fc/Fc$^+$). All these data demonstrate the considerable potential utility of

---

(13) (a) Blount, J. F.; Finocchiaro, P.; Gust, D.; Mislow, K. *J. Am. Chem. Soc.* **1973**, *95*, 7019. (b) Yamaguchi, S.; Akiyama, S.; Tamao, K. *J. Am. Chem. Soc.* **2000**, *122*, 6335.

(14) Sakamoto, Y.; Suzuki, T.; Miura, A.; Fujikawa, H.; Tokito, S.; Taga, Y. *J. Am. Chem. Soc.* **2000**, *122*, 1832.

(15) Theoretical calculations at the B3LYP/6-31G(d) level of theory showed that *B,B′,B″*-tris(10-diphenylboryl-9-anthryl)-*N,N′,N″*-tris(*p*-methylphenyl)-borazine (a model for **7**; KS LUMO, −1.74 eV) and Alq$_3$ (KS LUMO, −1.73 eV) have their LUMO at comparable energy level to each other.

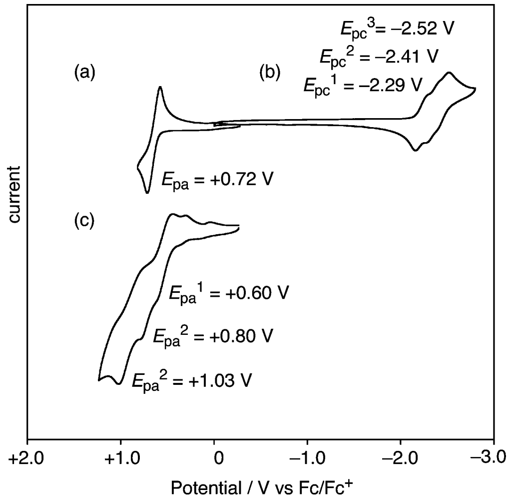

Figure 7. Cyclic voltammograms of (a) **7** in CH_2Cl_2, (b) **7** in THF, and (c) **8** in CH_2Cl_2, measured with $Bu_4N^+ClO_4^-$ (0.1 M) as a supporting electrolyte at a scan rate of 100 mVs^{-1}.

trianthrylborazine as a core framework for electronic device applications.

Conclusion

We here disclosed a new molecular design for cumulative π-electron systems, namely, π-conjugated molecule bundles exploiting borazine as a hexagonal core skeleton. As a prototype, a series of *B*,*B*′,*B*′′-trianthryl-*N*,*N*′,*N*′′-triarylborazines was synthesized in a facile one-pot procedure. On the basis of their C_3 symmetrical gear-shaped molecular structures, these compounds form characteristic two-dimensional honeycomblike networks, which consist of offset face-to-face intermolecular π-stacking of the anthracene moieties. These structures might be suitable for achieving high carrier-transporting abilities; thus, their application in this area is our next subject for investigation. In addition, the elucidation of the properties of these compounds demonstrates distinct bundle effects on their electronic structures and thus on their photophysical and electrochemical properties, such as the enhancement of fluorescence intensity and the possibility of tuning oxidation potential. These results suggest the great potential of this design in the creation of excellent new π-electron materials. Expanding on this molecular design, our current work involves the introduction of more extended π-conjugated frameworks in place of the anthracenes.

Experimental Section

General Procedure. Melting points (mp) were measured on a Yanaco MP-S3 instrument. ^{1}H and ^{13}C NMR spectra were measured with a JEOL A-400 spectrometer in $CDCl_3$ (400 MHz for ^{1}H and 100 MHz for ^{13}C). UV−vis absorption spectra and fluorescence spectra measurements were performed at room temperature with a Shimadzu UV-3150 spectrometer and a Hitachi F-4500 spectrometer, respectively, in a degassed spectral grade THF. Cyclic voltammetry (CV) was performed on an ALS/chi-617A electrochemical analyzer. The CV cell consisted of a glassy carbon electrode, a Pt wire counter electrode, and an Ag/AgNO$_3$ reference electrode. The measurements were carried out under argon atmosphere using CH_2Cl_2 or THF solutions of samples with a concentration of 1 mM and 0.1 M tetrabutylammonium perchlorate as a supporting electrolyte. The redox potentials were calibrated with ferrocene as an internal standard. Thin-layer chromatography (TLC) was performed on plates coated with 0.25-mm thick silica gel 60F-254 (Merck). Column chromatography was performed using Kieselgel 60 (70−230 mesh; Merck). All experiments were carried out under argon atmosphere.

Computational Method. All calculations were conducted using the Gaussian 98 program.[16]

***B*,*B*′,*B*′′-Tri(9-anthryl)-*N*,*N*′,*N*′′-tris(*p*-hexylphenyl)borazine (1).** To a solution of BCl_3 (1 M, 7.20 mL, 7.20 mmol) in hexane, a solution of 4-hexylaniline (1.00 g, 5.65 mmol) in toluene (7.5 mL) was added dropwise at 0 °C. The mixture was refluxed for 19 h to give a solution containing *N*,*N*′,*N*′′-tris(4-hexylphenyl)-*B*,*B*′,*B*′′-trichloroborazine. This solution was added to a THF solution (12 mL) of 9-lithioanthracene at 0 °C via cannula, which was prepared from 9-bromoanthracene (1.45 g, 5.65 mmol) with *t*-BuLi (1.47 M in pentane, 7.7 mL, 11.3 mmol) in THF at −78 °C. The mixture was allowed to warm to room temperature and was stirred for 20 h. After addition of 10 mL of water, the organic layer was separated, and the aqueous layer was extracted three times with $CHCl_3$. The combined organic layer was dried over $MgSO_4$, filtered, and evaporated under reduced pressure. The mixture was purified by a silica gel column chromatography (5:2 hexane/toluene, $R_f = 0.40$) to give 1.43 g (1.31 mmol) of **1** in 70% yield as yellow solids: mp 282−283 °C; ^{1}H NMR ($CDCl_3$) δ 8.44 (d, $J_{HH} = 8.4$ Hz, 6H), 7.96 (s, 3H), 7.70 (d, $J_{HH} = 8.4$ Hz, 6H), 7.59 (t, $J_{HH} = 8.4$ Hz, 6H), 7.32 (t, $J_{HH} = 8.4$ Hz, 6H), 6.57 (d, $J_{HH} = 8.4$ Hz, 6H), 5.77 (d, $J_{HH} = 8.4$ Hz, 6H), 1.73 (t, $J_{HH} = 7.2$ Hz, 6H), 1.10−0.76 (m, 27 H), 0.52−0.45 (m, 6H); ^{13}C NMR ($CDCl_3$) δ 142.6, 143.7, 137.5 (br), 132.9, 130.5, 129.4, 128.5, 126.3, 126.2, 126.0, 124.3, 124.2, 34.2, 31.4, 30.2, 27.5, 22.4, 14.1; FAB MS *m*/*z* 1089 (M$^+$). Anal. Calcd for $C_{78}H_{78}B_3N_3$: C, 85.96; H, 7.21; N, 3.86. Found: C, 85.69; H, 7.16; N, 4.03.

***B*,*B*′,*B*′′-Tri(9-anthryl)-*N*,*N*′,*N*′′-tris(*p*-isopropylphenyl)borazine (2).** This compound was prepared essentially in the same manner as described for **1** using 4-isopropylaniline as a starting material. The purification by a silica gel column chromatography (3:2 hexane/toluene, $R_f = 0.40$) gave 4.85 g (5.03 mmol) of **2** in 52% yield as yellow solids: mp > 300 °C; ^{1}H NMR ($CDCl_3$) δ 8.38 (d, $J_{HH} = 8.4$ Hz, 6H), 7.94 (s, 3H), 7.68 (d, $J_{HH} = 8.4$ Hz, 6H), 7.55 (t, $J_{HH} = 8.4$ Hz, 6H), 7.30 (t, $J_{HH} = 8.4$ Hz, 6H), 6.51 (d, $J_{HH} = 8.4$ Hz, 6H), 5.77 (d, $J_{HH} = 8.4$ Hz, 6H), 2.00 (sep, $J_{HH} = 6.8$ Hz, 3 H), 0.47 (d, $J_{HH} = 6.8$ Hz, 18H); ^{13}C NMR ($CDCl_3$) δ 143.9, 142.7, 133.0, 130.6, 129.5, 128.4, 126.4, 126.1, 124.3, 124.2, 123.8, 32.6, 23.2 (one peak for the carbon atoms bonding to the boron atoms is not observed due to quadrupolar relaxation); EI MS *m*/*z* 963 (M$^+$). Anal. Calcd for $C_{69}H_{60}B_3N_3$: C, 86.00; H, 6.28; N, 4.36. Found: C, 85.81; H, 6.17; N, 4.43.

***B*,*B*′,B′′-Tri(9-anthryl)-*N*,*N*′,N′′-tris[*p*-(trifluoromethyl)phenyl]borazine (3).** This compound was prepared essentially in the same manner as described for **1** using 4-trifluoromethylaniline as a starting material. The purification by a silica gel column chromatography (3:2 hexane/toluene, $R_f = 0.25$) gave 3.52 g (3.38 mmol) of **3** in 33% yield as pale yellow solids: mp > 300 °C; ^{1}H NMR ($CDCl_3$) δ 8.30 (d, $J_{HH} = 8.4$ Hz, 6H), 8.05 (s, 3H), 7.75 (d, $J_{HH} = 8.4$ Hz, 6H), 7.63 (t, $J_{HH} = 8.4$ Hz, 6H), 7.36 (t, $J_{HH} = 8.4$ Hz, 6H), 6.78 (d, $J_{HH} = 8.4$ Hz, 6H), 6.28 (d, $J_{HH} = 8.4$ Hz, 6H); ^{13}C NMR ($CDCl_3$) δ 147.9, 134.7 (br), 132.7, 130.5, 129.2, 128.0, 127.6, 126.7, 126.5, 125.4, 124.7, 124.6, 123.4 (q); EI MS *m*/*z* 1041 (M$^+$). Anal. Calcd for $C_{63}H_{39}B_3F_9N_3$: C, 72.66; H, 3.77; N, 4.03. Found: C, 72.46; H, 3.80; N, 4.17.

***B*,*B*′,*B*′′-Tri(9-anthryl)-*N*,*N*′,*N*′′-tributylborazine (4).** This compound was prepared essentially in the same manner as described for **1** using butylamine as a starting material. The purification by a silica gel column chromatography (3:1 hexane/$CHCl_3$, $R_f = 0.50$) gave 0.717 g (0.922 mmol) of **4** in 48% yield as colorless solids: mp > 300 °C; ^{1}H NMR ($CDCl_3$) δ 8.40 (s, 3H), 8.24 (d, $J_{HH} = 8.4$ Hz, 6H), 8.00 (d, $J_{HH} = 8.4$ Hz, 6H), 7.60 (t, $J_{HH} = 8.4$ Hz, 6H), 7.47 (t, $J_{HH} = 8.4$ Hz, 6H), 2.62−2.58 (m, 6H), 0.85−0.77 (m, 6H), −0.13 (sex, $J_{HH} = 7.2$ Hz, 6H), −0.53 (t, $J_{HH} = 7.4$ Hz, 9H); ^{13}C NMR ($CDCl_3$) δ 133.5, 131.3, 129.1, 128.9, 126.6, 125.1, 125.0, 48.8, 35.6, 19.3, 12.1 (one peak for

---

(16) Frisch, M. J., et al. A. *Gaussian 98*, revision A.5; Gaussian, Inc.: Pittsburgh, PA, 1998.

the carbon atoms bonding to the boron atoms is not observed due to quadrupolar relaxation); FAB MS *m*/*z* 778 (M+H$^+$). Anal. Calcd for $C_{54}H_{54}B_3N_3$: C, 83.42; H, 7.00; N, 5.40. Found: C, 83.64; H, 7.07; N, 5.41.

***B*,*B*′,*B*′′-Tris(10-bromo-9-anthryl)-*N*,*N*′,*N*′′-tris(*p*-hexylphenyl)-borazine derivative (5).** To a solution of BCl_3 (1 M, 21.7 mL, 21.7 mmol) in hexane, a solution of 4-hexylaniline (2.96 g, 16.7 mmol) in toluene (20 mL) was added dropwise at 0 °C. After addition of the solution of the aniline derivative, the mixture was refluxed for 15 h to give a solution containing *N*,*N*′,*N*′′-tris(*p*-hexylphenyl)-*B*,*B*′,*B*′′-trichloroborazine. This solution was added to a THF solution (65 mL) of 10-bromo-9-anthryllithium at 0 °C via cannula, which was prepared from 9,10-dibromoanthracene (5.63 g, 16.8 mmol) with *n*-BuLi (1.60 M in hexane, 10.5 mL, 16.8 mmol) in THF at −78 °C. The mixture was gradually warmed to room temperature and was stirred for 20 h. After the addition of 50 mL of water, the organic layer was separated, and the aqueous layer was extracted three times with $CHCl_3$. The combined organic layer was dried over $MgSO_4$, filtered, and evaporated under reduced pressure. The mixture was purified by a silica gel column chromatography (5:1 hexane/toluene, $R_f = 0.20$) to give 5.15 g (3.88 mmol) of **5** in 70% yield as pale yellow solids: mp 186−188 °C; ^{1}H NMR ($CDCl_3$) δ 8.40 (d, $J_{HH} = 8.4$ Hz, 6H), 8.26 (d, $J_{HH} = 8.4$ Hz, 6H), 7.63 (t, $J_{HH} = 8.4$ Hz, 6H), 7.45 (t, $J_{HH} = 8.4$ Hz, 6H), 6.48 (d, $J_{HH} = 8.4$ Hz, 6H), 5.77 (d, $J_{HH} = 8.4$ Hz, 6H), 1.74 (t, $J_{HH} = 7.2$ Hz, 6H), 1.07−1.00 (m, 6H), 0.95−0.88 (m, 6H), 0.83−0.78 (m, 6H), 0.75 (t, $J_{HH} = 7.2$ Hz, 9 H), 0.56−0.48 (m, 6H); ^{13}C NMR ($CDCl_3$) δ 142.0, 138.5, 137.9 (br), 133.5, 129.6, 129.4, 128.0, 126.4, 126.2, 126.1, 124.7, 122.7, 34.2, 31.3, 30.3, 27.6, 22.4, 14.1. Anal. Calcd for $C_{78}H_{75}B_3Br_3N_3$: C, 70.62; H, 5.70; N, 3.17. Found: C, 70.90; H, 5.75; N, 3.31.

***N*,*N*′,*N*′′-Tris(*p*-hexylphenyl)-*B*,*B*′,*B*′′-tris(10-diisopropylsilyl-9-anthryl)borazine (6).** To a solution of **5** (401 mg, 0.303 mmol) in THF (2 mL) cooled at −78 °C was added *t*-BuLi (1.47 M in pentane, 1.25 mL, 1.84 mmol) dropwise. After the mixture was stirred at −78 °C for 1 h, diisopropylsilyl chloride (150 mg, 1.00 mmol) was added to the mixture at −30 °C. The reaction mixture was gradually warmed to room temperature and stirred for 20 h. After addition of 1 M $NaHCO_3$ aqueous solution, the organic layer was separated, and the aqueous layer was extracted three times with CH_2Cl_2. The combined organic layer was dried over $MgSO_4$, filtered, and evaporated under reduced pressure. The mixture was purified by a silica gel column chromatography (5:1 hexane/toluene, $R_f = 0.23$) to give 199 mg (0.139 mmol) of **6** in 46% yield as colorless solids: mp 208−210 °C; ^{1}H NMR ($CDCl_3$) δ 8.46 (d, $J_{HH} = 8.4$ Hz, 6H), 8.24 (d, $J_{HH} = 8.4$ Hz, 6H), 7.55 (t, $J_{HH} = 8.4$ Hz, 6H), 7.31 (t, $J_{HH} = 8.4$ Hz, 6H), 6.51 (d, $J_{HH} = 8.4$ Hz, 6H), 5.73 (d, $J_{HH} = 8.4$ Hz, 6H), 4.63 (t, $J_{HH} = 4.8$ Hz, 3H), 1.62 (t, $J_{HH} = 7.2$ Hz, 6H), 1.47−1.40 (m, 6H), 1.13 (d, $J_{HH} = 7.6$ Hz, 18H), 1.06−1.04 (m, 3H), 1.04−1.01 (m, 6H), 0.92−0.88 (m, 6H), 0.77−0.72 (m, 3H), 0.74 (t, $J_{HH} = 7.6$ Hz, 9H), 0.63 (m, 6H), 0.56 (d, $J_{HH} = 7.6$ Hz, 18H); ^{13}C NMR ($CDCl_3$) δ 142.4, 140.8 (br), 137.9, 136.5, 132.4, 131.3, 130.6, 128.9, 126.3, 125.8, 124.1, 123.6, 34.4, 31.3, 30.4, 28.2, 22.3, 20.4, 19.4, 14.0, 13.5; FAB MS *m*/*z* 1432.44 (M+H$^+$); HRMS calcd for $C_{96}H_{121}B_3N_3Si_3$, 1432.9186; found, 1432.9204.

***N*,*N*′,*N*′′-Tris(*p*-hexylphenyl)-*B*,*B*′,*B*′′-tris(10-dimesitylboryl-9-anthryl)borazine (7).** To a solution of **5** (427 mg, 0.322 mmol) in THF (3 mL) cooled at −78 °C was added *t*-BuLi (1.46 M in pentane, 1.35 mL, 1.97 mmol) dropwise. After the mixture was stirred at −78 °C for 1 h, dimesitylfluoroborane (389 mg, 1.45 mmol) was added to the mixture at −78 °C. The reaction mixture was gradually warmed to room temperature and stirred for 27 h. After addition of 3 mL of water, the organic layer was separated, and the aqueous layer was extracted three times with $CHCl_3$. The combined organic layer was dried over $MgSO_4$, filtered, and evaporated under reduced pressure. The mixture was purified by a silica gel column chromatography (2:1 hexane/toluene, $R_f = 0.30$) to give 201 mg (0.109 mmol) of **7** in 34% yield as yellow solids: mp > 300 °C; ^{1}H NMR ($CDCl_3$) δ 8.42 (d, $J_{HH} = 8.4$ Hz, 6H), 7.77(d, $J_{HH} = 8.4$ Hz, 6H), 7.45 (br, 6H), 7.05 (t, $J_{HH} = 8.4$ Hz, 6H), 6.78 (s, 6H), 6.58 (d, $J_{HH} = 8.4$ Hz, 6H), 6.48 (s, 6H), 5.79 (d, $J_{HH} = 8.4$ Hz, 6H), 2.21 (s, 18H), 2.03 (s, 18H), 1.80 (t, $J_{HH} = 8.0$ Hz, 6H), 1.15 (s, 18H), 1.15−1.03 (m, 6H), 1.01−0.97 (m, 6H), 0.92−0.88 (m, 6H), 0.83−0.78 (m, 6H), 0.76 (t, $J_{HH} = 7.2$ Hz, 9H); ^{13}C NMR ($CDCl_3$) δ 145.6, 145.5, 142.6, 141.3, 141.1 (br), 140.3, 139.4, 137.8, 132.7, 132.4, 130.4, 128.8, 128.7, 128.5, 126.5, 125.9 (br), 124.2, 123.9, 34.7, 31.6, 30.6, 28.7, 23.3, 23.0, 22.5, 21.2, 14.1; MALDI-TOF MS *m*/*z* 1836 (M$^+$). Anal. Calcd for $C_{132}H_{141}B_6N_3$: C, 86.43; H, 7.75; N, 2.29. Found: C, 86.16; H, 7.75; N, 2.35.

***N*,*N*′,*N*′′-Tris(*p*-hexylphenyl)-*B*,*B*′,*B*′′-tris{10-[*p*-(*N*,*N*-diphenylamino)phenyl]-9-anthryl}borazine (8).** To a solution of **5** (403 mg, 0.304 mmol) in THF (2 mL) cooled at −78 °C was added *t*-BuLi (1.47 M in pentane, 1.25 mL, 1.84 mmol) dropwise. After the mixture was stirred at −78 °C for 1 h, $ZnCl_2$(tmen) (230 mg, 0.91 mmol) (tmen: *N*,*N*,*N*′,*N*′-tetramethylethylenediamine) was added to the mixture at 0 °C. The reaction mixture was stirred at 0 °C for additional 2 h. *p*-Bromo(*N*,*N*′-diphenylamino)benzene (326 mg, 1.01 mmol) and Pd-$(PPh_3)_4$ (35.5 mg, 0.0307 mmol) were added to the mixture under a stream of argon gas. The reaction mixture was refluxed for 24 h. After addition of 2 mL of water, the organic layer was separated, and the aqueous layer was extracted with $CHCl_3$ three times. The combined organic layer was dried over $MgSO_4$, filtered, and evaporated under reduced pressure. The mixture was purified by a silica gel column chromatography (3:2 hexane/toluene, $R_f = 0.25$) to give 133 mg (0.073 mmol) of **8** in 24% yield as yellow solids: mp 184−186 °C; ^{1}H NMR ($CDCl_3$) δ 8.48 (d, $J_{HH} = 8.4$ Hz, 6H), 7.58 (t, $J_{HH} = 8.4$ Hz, 6H), 7.51 (d, $J_{HH} = 8.4$ Hz, 6H), 7.25 (t, $J_{HH} = 8.4$ Hz, 6H), 7.24 (t, $J_{HH} = 8.4$ Hz, 12H), 7.17 (d, $J_{HH} = 8.4$ Hz, 12 H), 7.13 (d, $J_{HH} = 8.4$ Hz, 6H), 7.00 (t, $J_{HH} = 8.4$ Hz, 6H), 6.98 (d, $J_{HH} = 8.4$ Hz, 6H), 6.59 (d, $J_{HH} = 8.4$ Hz, 6H), 5.81 (d, $J_{HH} = 8.4$ Hz, 6H), 1.75 (t, $J_{HH} = 7.2$ Hz, 6H), 1.00−0.94 (m, 6H), 0.90−0.80 (m, 12H), 0.65 (t, $J_{HH} = 7.2$ Hz, 9H), 0.63−0.58 (m, 6H); ^{13}C NMR ($CDCl_3$) δ 147.8, 146.6, 142.8, 137.8, 136.4, 133.1, 132.8, 132.1, 129.7, 129.2, 129.2, 127.1, 126.4, 126.0, 124.3, 124.2, 124.1, 123.1, 122.8, 34.5, 31.5, 30.8, 28.0, 22.3, 14.0 (one peak for the carbon atoms bonding to the boron atoms is not observed due to quadrupolar relaxation); MALDI-TOF MS *m*/*z* 1819 (M$^+$). Anal. Calcd for $C_{132}H_{117}B_3N_6$: C, 87.12; H, 6.48; N, 4.62. Found: C, 87.11; H, 6.42; N, 4.59.

X-ray Crystal Structure Analysis of Compound 2. Single crystals of **2** suitable for X-ray crystal analysis were obtained by slow diffusion of hexane into a solution of **2** in toluene. Intensity data were collected at 100 K on a Bruker SMART APEX diffractometer with Mo Kα radiation ($\lambda = 0.71073$ Å) and a graphite monochromator. A total of 15190 reflections were measured at a maximum 2θ angle of 50.0°, of which 10215 were independent reflections ($R_{int} = 0.0226$). The structure was solved by direct methods (SHELXS-97[17]) and refined by the full-matrix least-squares on F^2 (SHELXL-97[17]). All non-hydrogen atoms were refined anisotropically, and all hydrogen atoms were placed using AFIX instructions. Two solvent molecules of toluene were included in a lattice. The crystal data are as follows: $C_{76}H_{68}B_3N_3$; FW = 1055.76, crystal size 0.30 × 0.30 × 0.30 mm^3, Triclinic, *P*-1, $a = 10.0274(9)$ Å, $b = 15.5465(14)$ Å, $c = 20.3707(18)$ Å, $\alpha = 69.938(2)°$, $\beta = 87.374(2)°$, $\gamma = 83.796(2)°$, $V = 2965.3(5)$ Å^3, $Z = 2$, $D_c = 1.182$ g cm^{-3}. The refinement converged to $R_1 = 0.0457$, w$R_2 = 0.0981$ ($I > 2\sigma(I)$), GOF = 0.899.

X-ray Crystal Structure Analysis of Compound 3. Single crystals of **3** suitable for X-ray crystal analysis were obtained by slow diffusion of hexane into a solution of **3** in toluene. Intensity data were collected at 100 K on a Bruker SMART APEX diffractometer with Mo Kα radiation ($\lambda = 0.71073$ Å) and a graphite monochromator. A total of 19059 reflections were measured at a maximum 2θ angle of 56.5°, of which 4754 were independent reflections ($R_{int} = 0.1451$). The structure was solved by direct methods (SHELXS-97[17]) and refined by the full-

---

(17) Sheldrick, G. M. *SHELX-97, Program for the Refinement of Crystal Structures*; University of Gottingen: Gottingen, Germany, 1997.

matrix least-squares on F^2 (SHELXL-97[17]). The CF_3 group was disordered. Two sets of fluorines, that is, F1−F3 and F4−F6, were placed and their occupancies were refined to be 0.60 and 0.40, respectively. The disordered solvent molecules of nine toluenes and three hexanes were included in a lattice. The toluene molecule (C22, C22*, C23, C23*, C24, C24*, C25, C25*) sits on a 2-fold rotation axis. Thus, the disordered methyl group of C25 was placed with fixed occupancy value of 0.50. On the other hand, the hexane molecule (C26, C27, C28, C26*, C27*, C28*) sits on a 3-fold rotation axis. The disordered carbons of C26−C28 were placed with the fixed occupancy value of 0.33. All non-hydrogen atoms were refined anisotropically. All hydrogen atoms, except for those of disordered hexane (C26−C28), were placed using AFIX instructions. The crystal data are as follows: $C_{76.5}H_{51}B_3F_9N_3$; FW = 1215.63, crystal size 0.30 × 0.30 × 0.30 mm^3, Trigonal, R-3, $a = b = 20.4905(10)$ Å, $c = 25.5846(17)$ Å, $\alpha = \gamma = 90°$, $\beta = 120°$, $V = 9302.8(9)$ Å^3, $Z = 6$, $D_c = 1.302$ g cm^{-3}. The refinement converged to $R_1 = 0.0808$, $wR_2 = 0.2217$ ($I > 2\sigma(I)$), GOF = 1.071.

Acknowledgment. We thank Professor Koichi Komatsu of Kyoto University for use of the X-ray diffractometer. This work was supported by Grants-in-Aid (No.12CE2005 for Elements Science, and No. 16750031) from the Ministry of Education, Culture, Sports, Science, and Technology, Japan.

Supporting Information Available: X-ray structure of **2**; calculated molecular coordinates of **1′**, **3**, and **4′** at the B3LYP/6-31G(d) level of theory (PDF). X-ray crystallographic files of **2** and **3** (CIF). This material is available free of charge via the Internet at http://pubs.acs.org.

JA0537171